

# $\text{Pr}_x\text{Ce}_{1-x}\text{O}_{2-\delta}$ as a functional material for SOCs

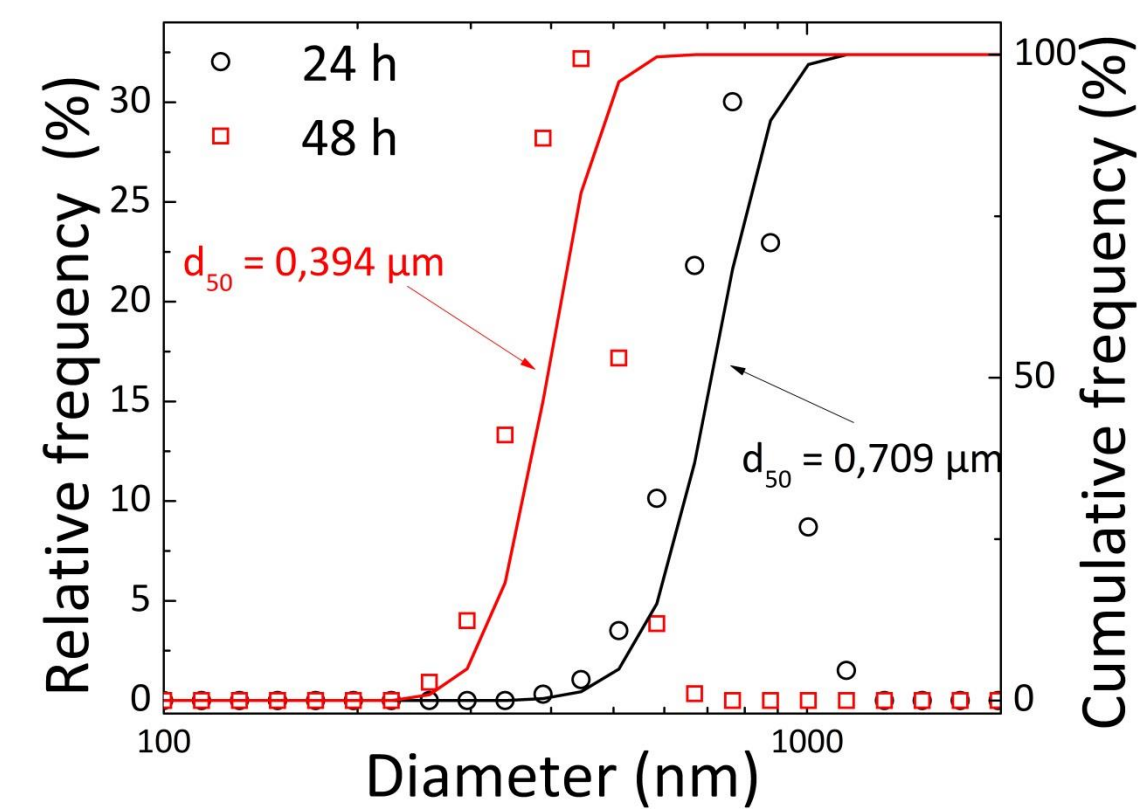
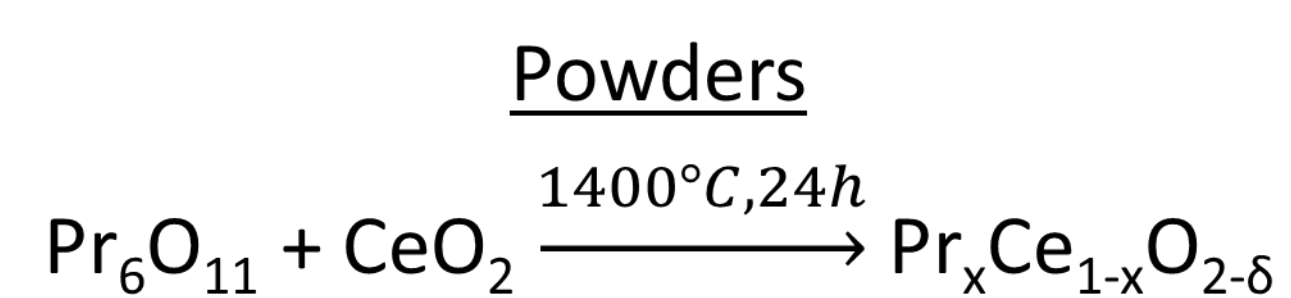
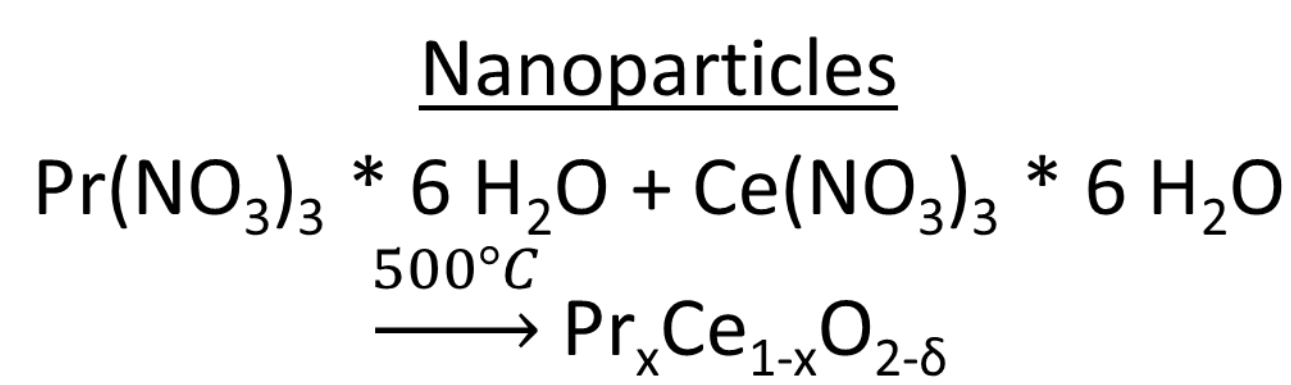
C. Lenser<sup>1</sup>, F. Gunkel<sup>2</sup>, N.H. Menzler<sup>1</sup> and O. Guillon<sup>1,3</sup><sup>1</sup> Institute of Energy and Climate Research - Materials Synthesis and Processing (IEK-1), Forschungszentrum Jülich GmbH, 52425 Jülich, Germany<sup>2</sup> Institute for Electronic Materials (IWE2), RWTH Aachen University, 52074 Aachen, Germany<sup>3</sup> Jülich Aachen Research Alliance: JARA-Energy

## Introduction

Solid oxide cells (SOCs) offer the possibility to reversibly convert fuel (such as  $\text{H}_2$  or  $\text{CH}_4$  gas) into electricity (fuel cells) or electricity into fuel (electrolyzers). Gadolinium-doped ceria (GDC) is currently used as a Sr-diffusion barrier in state-of-the-art anode supported cells (ASC), and is investigated as an electrolyte for low-temperature applications. In contrast to GDC, Praseodymium-doped ceria (PCO) is a mixed ionic-electronic conductor (MIEC) in air due to the mixed  $\text{Pr}^{3+}/\text{Pr}^{4+}$  valence state, and therefore interesting as an active component on the air side of SOCs. It has been suggested from work on model systems that PCO could show a comparable performance to  $\text{La}_{0.58}\text{Sr}_{0.4}\text{Co}_{0.2}\text{Fe}_{0.8}\text{O}_{3-\delta}$  (LSCF).<sup>1</sup> In the present work, we investigate the structural and electrochemical properties of PCO ceramics, as well the performance as an alternate cathode material and Sr-diffusion barrier for the use in SOCs.

<sup>1</sup>: D. Chen et al., J. Electroceram (2012), 28:62-69

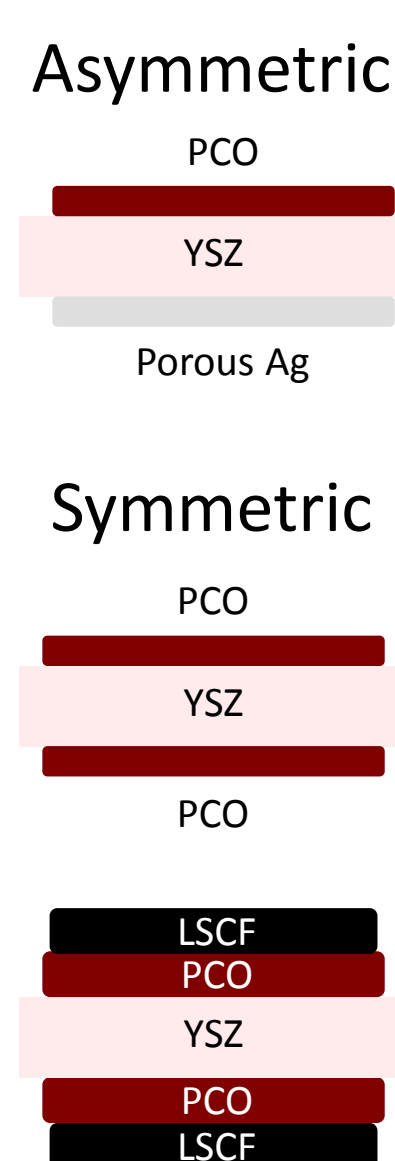
## Synthesis and Processing



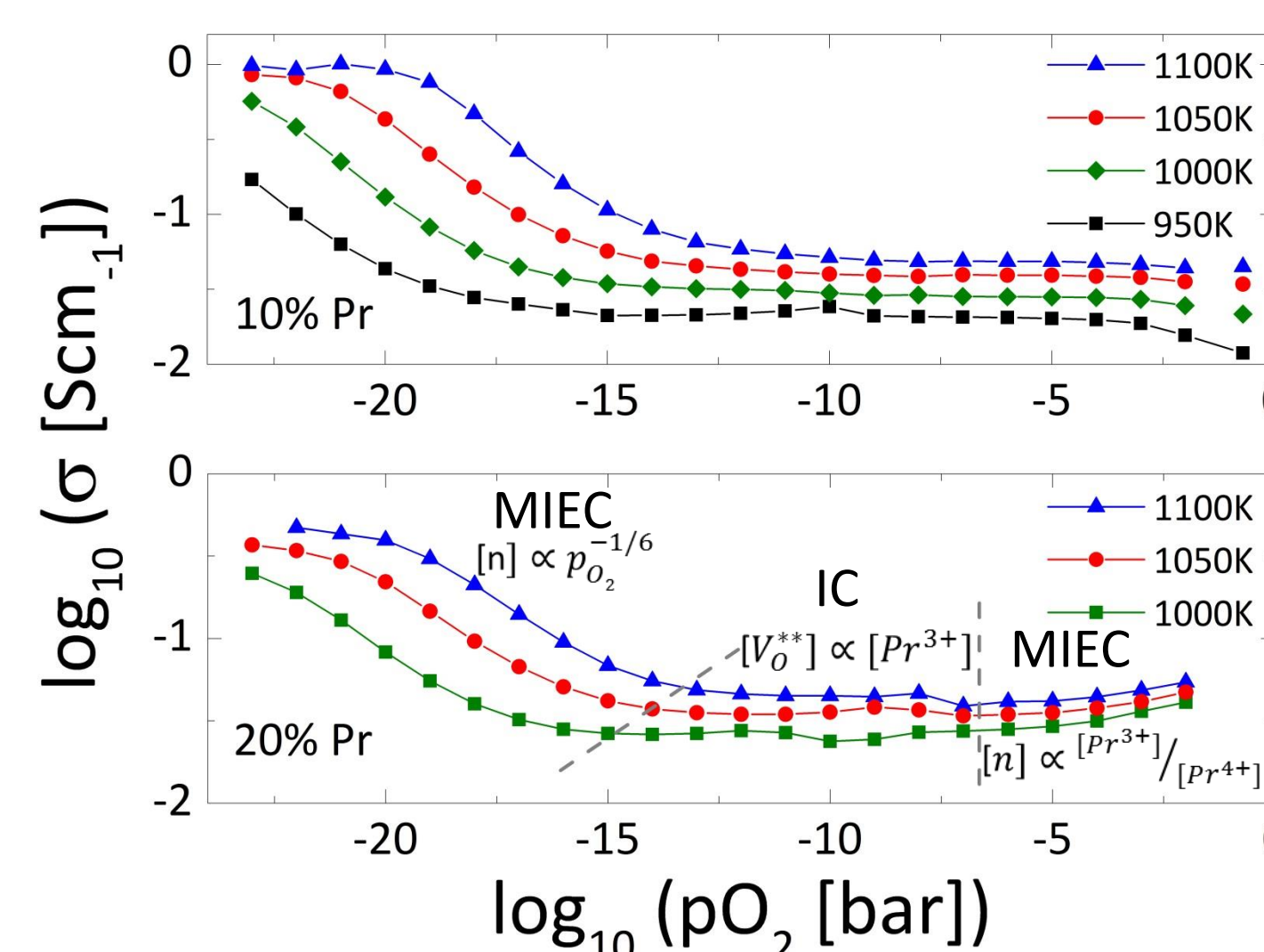
Particle-size distribution of solid-state prepared powders after milling

Powders were ground in a mortar and ball milled (3 mm YSZ balls) in EtOH for 24 and 48 hours, respectively. Dynamic laser scattering (DLS) was used to investigate the particle size distribution.

Screen printing pastes were prepared by homogenizing the powders in terpineol and mixing the pre-suspension with ethylcellulose solved in terpineol. Layers were printed on 150  $\mu\text{m}$  8YSZ foils (Kerafol), using a circular geometry with  $\varnothing = 12$  mm for PCO and  $\varnothing = 10$  mm for LSCF. Symmetric and asymmetric cells were prepared for EIS and microscopy.



## Material properties

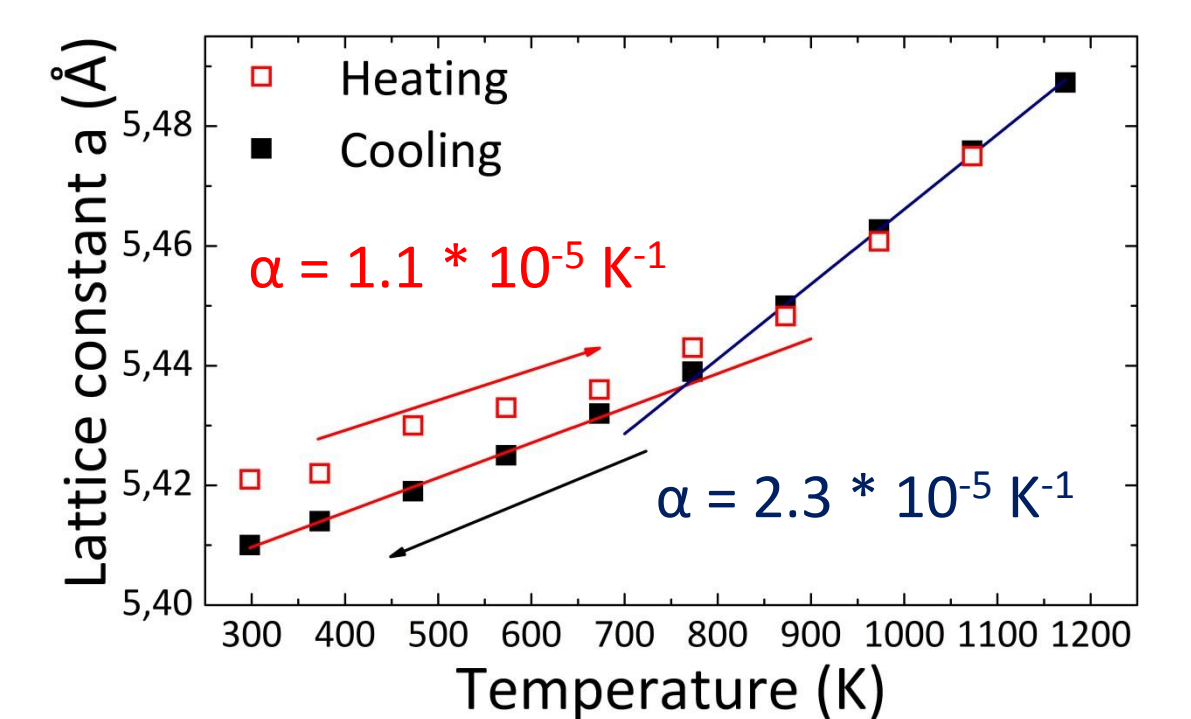
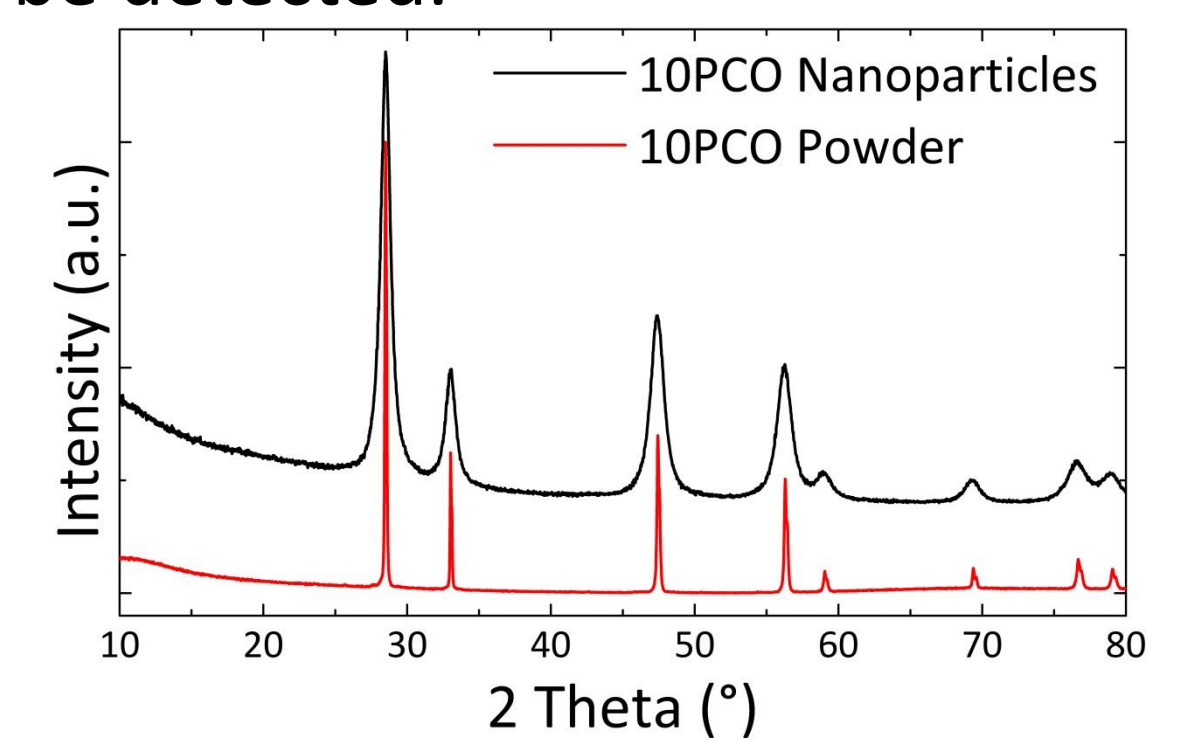


The DC-conductivity of 10% and 20% Pr-doped  $\text{CeO}_2$  was investigated via 4-point measurements in a temperature and atmosphere controlled environment.

The three observed regimes correspond to an MIEC behavior at high  $p\text{O}_2$ , an ionic plateau at intermediate  $p\text{O}_2$  values and electronic conduction at low  $p\text{O}_2$  due to the reduction of  $\text{Ce}^{4+} \rightarrow \text{Ce}^{3+}$  ions, in agreement with prior reports.<sup>2</sup>

<sup>2</sup>: Bishop et al., J. Mater. Res., Vol. 27, No. 15, Aug 14, 2012<sup>3</sup>: D. Balzar et al., J. Appl. Cryst. (2004). 37, 911-924

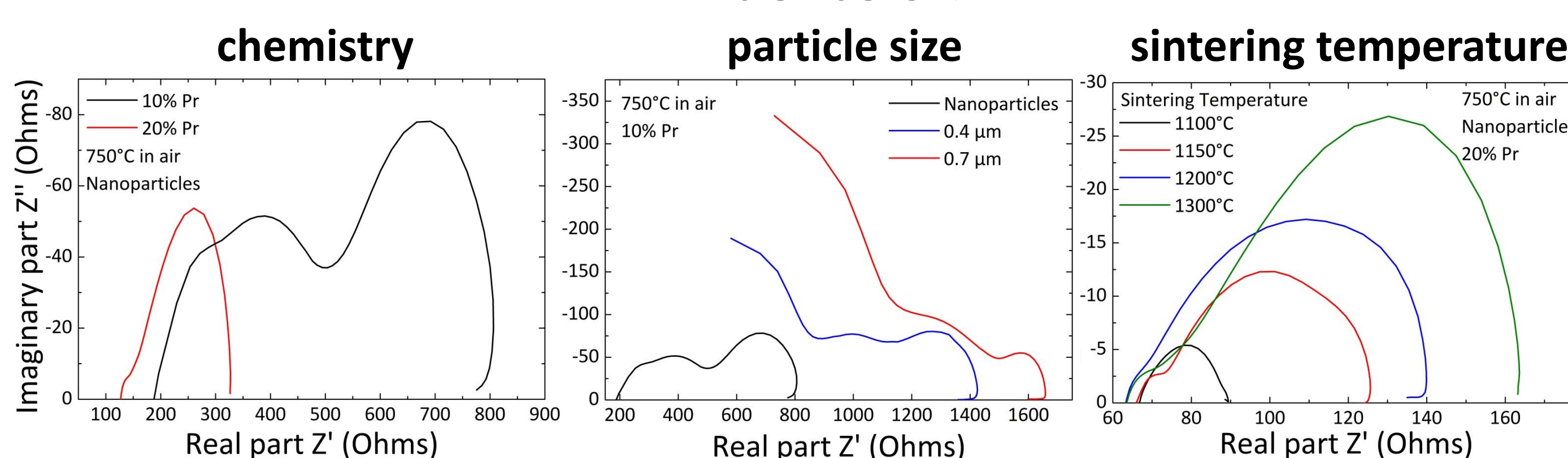
The grain size after synthesis of the nanopowder is 6.5 nm as determined by X-ray diffraction (XRD).<sup>3</sup> No secondary phases can be detected.



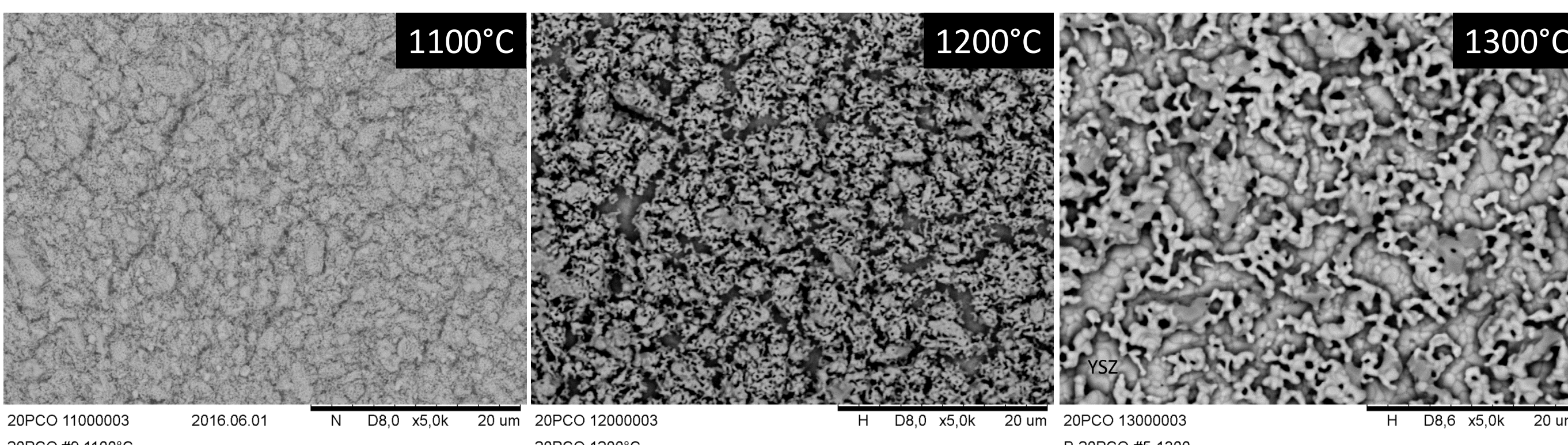
The chemical expansion of the 10PCO nanoparticles can be observed via *in-situ* XRD between 500°C and 600°C, demonstrating that oxygen exchange is active.

## Cathode performance

### Influence of:



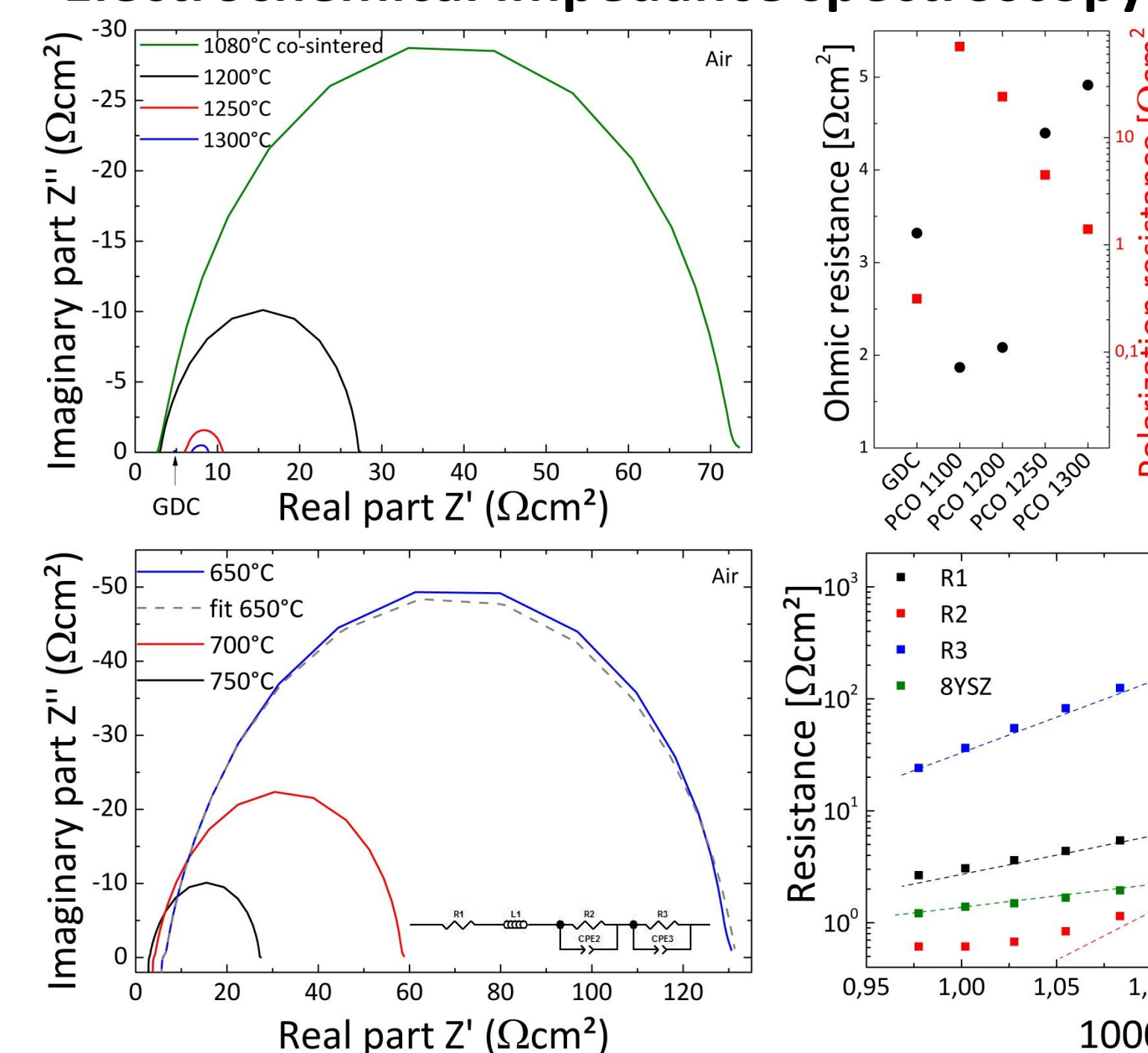
Electrochemical impedance spectroscopy (EIS) in air is used to assess the cathode performance of porous  $\text{Pr}_{1-x}\text{Ce}_x\text{O}_{2-\delta}$  layers. Systematic dependency of the polarization resistance on chemistry and microstructure can be evaluated without a detailed understanding of the underlying processes.



Microstructure control through tailored primary particle size and sintering conditions is the key to optimize cathode performance for a given chemistry. Cathode performance increases with increased Pr-content (polaron concentration) and with decreased particle size and sintering temperature (larger inner surface area). These trends are in agreement with a surface exchange-limited cathode performance.

## Diffusion barrier

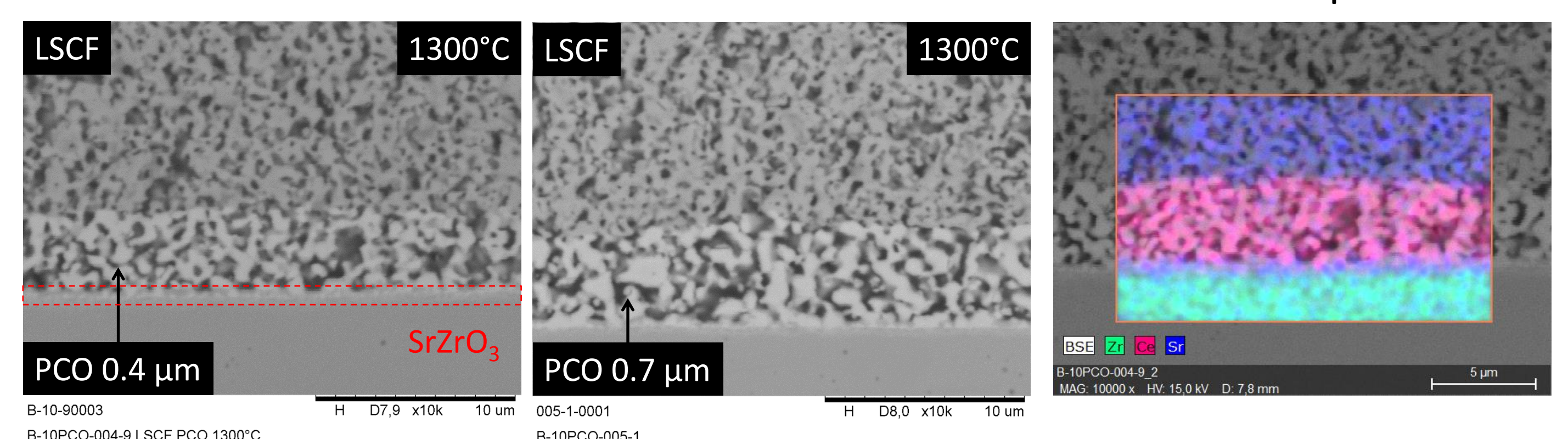
### Electrochemical impedance spectroscopy (EIS)



The ohmic resistance after cathode sintering shows a dependence on the sintering temperature of the PCO barrier layer. LSCF polarization resistance varies with LSCF thickness.

Cathode polarization is dominated by the oxygen surface exchange of LSCF,<sup>4</sup> modeled by a single RC-element. The activation energy  $E_A$  for the ohmic resistance  $R_1$  is close to the migration enthalpy of oxygen vacancies in doped ceria.<sup>5</sup>

### Microstructure



After cathode sintering, formation of  $\text{SrZrO}_3$  is observed for screen printed layers of both GDC and PCO.

<sup>4</sup>: Steele and Bae, Solid State Ionics 106 (1998) 255-261<sup>5</sup>: Bishop et al., Phys. Chem. Chem. Phys., 2011, 13, 10165-10173

## Conclusions

A facile synthesis using the low-temperature combustion of metal nitrates yields single-phase nanoparticles that show promising performance in EIS cathode testing. Layers printed with coarser powders show no significant activity toward oxygen reduction. Cathode performance is strongly influenced by the sintering temperature, as the nanoparticles agglomerate strongly during high temperature sintering.

Diffusion barrier layers made of PCO perform similar to GDC due to their porosity. Nanoparticle barriers co-sintered with the LSCF cathode at 1080°C exhibit low ohmic losses in the electrolyte. Further work is aimed at understanding the size effect of cathode performance and improving the density of sintered barrier layers.